

SAR AND LANDSAT TM IMAGE FUSION FOR LAND COVER CLASSIFICATION IN THE BRAZILIAN ATLANTIC FOREST DOMAIN

Claudio Azevedo Dupas

ITC, PO Box 6, 7500 AA Enschede, The Netherlands
cadupas@hotmail.com

KEY WORDS: Synthetic Aperture Radar (SAR), Landsat TM, Orthorectification, Image fusion, Gaussian maximum likelihood classification, Error matrix.

ABSTRACT

This paper demonstrates the applicability of Landsat TM and SAR image fusion for land cover classification in the Brazilian Atlantic forest domain. The Atlantic forest is considered one of the most threatened of the world's rain forest. Although Landsat TM has been used as an efficient tool for tropical forest monitoring, several problems remain. First, cloud cover is a constant problem in the tropics, which limits the vegetation cover assessments by the optical sensor. Second, forest, regrowth and clearings are not easily differentiated.

Recently, imaging radar satellites have been introduced to map natural resources. With long wavelengths, radar's radiation is not reflected or absorbed by clouds or haze, thereby allowing more frequent and systematic assessments of land cover changes and deforestation. The same principle allows penetrating in the canopy to assess data on the trunks level, which increases the potential of distinction between different stages of regrowth.

Two different SAR images were fused with a Landsat TM image using two different image fusion techniques. Image classification was performed and the classification accuracy was assessed. The classification accuracy from each fused image was compared the one from the Landsat TM. The best results were achieved by the image originated from combining the JERS-1 image with the Landsat TM image using the IHS cylindrical transformation. The results suggest that the image fusion Landsat TM / SAR could be an important alternative for land cover mapping in the Brazilian Atlantic forest domain.

1 INTRODUCTION

The Atlantic Forest, or 'Mata Atlantica', once covered more than a million square kilometers along the Brazilian coast. Its 'anthropogenic disturbance' began as soon as the colonists arrived, almost five centuries ago. The timber of 'Pau-brasil' (*Caesalpinia echinata*), commercially prized, was the forest's first major product and was logged almost to extinction. Afterwards, deforestation for sugarcane cultivation, mining, coffee, banana and rubber plantations also occurred as the settlers moved inland. This region is now the major agricultural and industrial area in Brazil and includes in its surrounding area over 100 million inhabitants. As a result, deforestation is still occurring and only 8.3 percent (SOS Mata Atlantica *et al.*, 1998) of the forest original area remains intact, irregularly distributed over fragments of different sizes, shapes and forest formations. 'These last vestiges of Atlantic forest are now considered to be one of the most threatened of the world's rain forests, sharing this distinction with the remains of the tropical forest in Madagascar' (IUCN, 1996). Recognizing its singularity and importance, in 1991 UNESCO declared the Atlantic forest as being a high priority area to create new biosphere reserves.

Although there are a considerable number of conservation areas in the Atlantic forest, the total area covered by parks, reserves and ecological stations amounts to only 3000 sq. km of the estimated 100,000 sq. km of actual forest area (IUCN, 1996). Based on these numbers, it's reasonable to say that the preservation of its remaining cover can only be achieved if new conservation areas are created. In order to indicate which parts of this unique biome are technically and strategically most important to be protected in a reserve, mapping and monitoring the land cover in a systematic and continuous way are needed. Moreover, precise numbers on the deforestation rate must be obtained.

Recently, a project has been implemented by INPE and the NGO SOS Mata Atlantica for continuously monitoring by quantifying the totality of the remaining forest using Landsat TM and with a five years temporal resolution. Up to now, the project generated two reports covering ten Federal States for the periods from 1985 to 1990 (SOS Mata Atlantica and INPE, 1993) and from 1990 to 1995 (SOS Mata Atlantica *et al.*, 1998). Both reports pointed cloud cover as being a constant problem, which led to gaps in all the maps and even to cancellation of the Bahia State map update.

For the last two decades, Landsat TM imagery has been used as an efficient tool for monitoring vegetation cover changes in tropical forest domains. Forest and clearings are well separated spectrally. Yet, several problems remain. First, the various stages of re-growth are not easily differentiated (Rignot *et al.*, 1997). Second, cloud cover is a constant problem in the humid tropics, which limits the vegetation cover assessments in time and space (Rignot *et al.*, 1997).

Since 1991, imaging radar has been used to map natural resources from satellite platforms (Lillesand and Kiefer, 1994). Differing from the optical, the SAR (Synthetic Aperture Radar) sensor is active, it emits and receives electromagnetic radiation using an antenna. The energy received back (or backscatter) depends on the target's roughness, shape, orientation towards the antenna, and moisture content. As the wavelengths used are in the order of a few centimetres to nearly 30 centimetres, the radiation is not reflected or absorbed by clouds or haze, thereby allowing more frequent and systematic assessments of land cover changes and deforestation. On the other hand, SAR imagery is usually affected by terrain geometric distortions on its side-scanning geometry causing layover, foreshortening and shadow (Pohl, 1996).

More recently, several studies have been conducted indicating the potential of merging optical and SAR data to assess better land cover classification results. In a study site located in the Brazilian amazon forest, Rignot *et al.*(1996) compared the classification results of two types of SAR sensors (SIR-C and JERS-1, with different wavelengths and incidence angles), two types of optical sensors (Landsat TM and Spot XS) and the combination of Landsat TM and SIR-C. They concluded the combined use of optical and radar imagery provides the most reliable form of land cover mapping, focusing on the discrimination of different stages of forest regrowth. Seven different classes of land cover including two levels of regrowth were mapped with 93% overall accuracy.

This study aims to evaluate the fusion of Landsat TM imagery with SAR satellite imaging data (from two different sensors, with different polarizations, wavelengths, and incidence angles) to assess land cover classification in a representative area of the Brazilian Atlantic forest domain.

2 STUDY AREA AND DATA SET

The study area is located in south-eastern Brazil, in the south-east of Minas Gerais State, approximately 150 km from Rio de Janeiro. It extends from 21°30' to 21°56' S and 43°40' and 44°13' W, with an area of about 20.75 ha. The region is part of the Mantiqueira mountain range and it is characterised by undulated terrain with occurrence of escarpments in some areas. The elevation varies from 700 to 1784 (Lombada peak) metres above sea level.

Based on the mentioned latitude and altitude above sea level, Veloso *et al.* (1991) and Oliveira-Filho and Ratter (1995) would classify the primary vegetation in study area as tropical montane semideciduous forest, one of the major Atlantic forest formations. It is described by the authors as being 'seasonal but moderately deciduous forest, occurring in the high-altitude (above 750m) hinterlands of southeastern and central Brazil, associated with soils of intermediate fertility'

Cattle grazing for milk production is the main land use type and therefore pasture is the dominant land cover type in the study area. *Eucalyptus* plantations occupy a secondary position in area but play an important role in the region's economy. Tourism has been increasing recently and is the main income for the population of Conceição do Ibitipoca, a village of about 1,000 inhabitants nearby the Ibitipoca State Park. Inaugurated in 1973, the park is centrally located in the study area and has the status of conservation area.

In data fusion, images have to be close to each other in time to avoid possible land cover changes. JERS-1 imagery was given a priority, since it is expected to give better forest cover classification results than the other available imaging SAR satellites due to its sensor characteristics (e.g. longer wavelength, medium incidence angle and HH polarization). The last JERS-1 image available for the region of interest is from December of 1995. The closest Landsat TM available with some clouds (not more than 10%) was chosen for data fusion purposes. An ERS-2 image was selected as a second source of SAR satellite data (with different sensor characteristics) for comparison purposes. A second Landsat TM image closer to the fieldwork date was selected to be classified for sampling design purposes. Finally, a cloud-free Landsat TM image was used as source of information on the cloud gaps from the first Landsat TM image. Table 1 shows the images and their correspondent specifications. The study area boundaries were defined by overlaying images from the different sources and evaluating the suitability of all possible areas that contained the three imagery types required.

Table 1: Satellite imagery selected, their main characteristics and purpose.

Product (#)	Date	Bands	Orbit/Path	Frame/Row	Scene Center	Pixel Size	Purpose
Landsat-5 TM (1)	24/08/95	3,4,5	218	075	21°41'S, 44°37'W	30m	data fusion
Landsat-5 TM (2)	31/01/96	3,4,5	218	075	21°40'S, 44°42'W	30m	cloud cover gaps info.
Landsat-5 TM (3)	16/08/98	3,4,5	218	075	21°42'S, 44°37'W	30m	sampling design
JERS-1. SAR. BSQ (4)	09/12/95	n.a.	377	337	21°83'S, 43°93'W	12.5m	data fusion
ERS-2. SAR. PRI (5)	17/04/96	n.a.	05188	4041	21°31'S, 43°47'W	12.5m	data fusion

The study area is covered by six 1:50,000 scale topographic map sheets produced by IBGE. The maps were edited in 1975 and are based on aerial photographs from 1966. These were the only cartographic information available containing this level of detail. The maps contain information on the roads and rail network, urban areas, municipalities, water bodies, land cover (just a few classes) and topography (20 metres spacing contour lines). The map projection used is the UTM zone 23K, based on the datum Corrego Alegre. Digital maps corresponding to the above-described set of map sheets were also obtained in order to build a DEM from the layer containing the contour lines.

3 METHODS

Following the stratified random sampling rules, four sets of sampling plots were measured during fieldwork. For the forest training set, 26 plots were measured; other 26 for the forest test set; 14 for the *Eucalyptus* training set and 14 for the *Eucalyptus* test set. For each plot, DBH, tree height, altitude, slope and aspect were measured. Only trees with height ≥ 3 m and DBH ≥ 10 cm were measured.

Two speckle filters were selected to be tested on JERS-1 and ERS-2 image subsets: the Gamma MAP filter (Lopes et al., 1993), and the Lee-Sigma filter (Lee, 1980). The filter algorithms are described in the above mentioned references. Three different window sizes (3x3, 5x5 and 7x7) were applied for each filter. A visual subjective judgement of the results pointed which one of the six filter-window combinations could best smooth the images while preserving the edges. The 5x5 Gamma Map was the one selected.

A raster DEM was produced from the 1:50,000-scale elevation vector layer (20m-spacing contour lines). The six topographic maps sheets covering the study area were scanned and rectified and a mosaic was created. The mosaic was used as 'master' image for rectification of all images.

Image fusion can only be performed if the pixels corresponding to the same location on the different images to be combined have the same size, orientation and center location. In other words, pixels registered to each other must refer to the same feature on the ground. Geometric correction, or geocoding, is therefore one of the most important steps in image fusion. Ortho-rectification is a geocoding system usually applied to correct remote sensing imagery (especially radar images) covering a mountainous area. It uses a geometric model to correct terrain-induced distortions. The following parameters are used in the model: platform (position, velocity, altitude), sensor (viewing geometry), map projection (coordinate system, datum, etc), Earth general parameters, and the final set of GCPs, defined by X, Y and Z (from a DEM) coordinates. The images were ortho-rectified using the OrthoEngine module of EASI/PACE software. Since the imagery used was going to be classified, the choices on which method to take were made on the basis of conserving as much as possible the original pixel values. The nearest neighbour was therefore the resample algorithm employed in image rectification. Moreover, in order to avoid multiple resampling (and therefore multiple changes in image geometry), image rectification, SAR speckle filtering, and the change in pixel size were all carried out in a single step. A common pixel size of 15 meters was used.

The previously rectified images were fused on a pixel-by-pixel basis. Each different type of SAR image was fused with the Landsat TM 95 image using two different fusion techniques. The different image combinations and transformation types are summarized in Table 2. Several have been described on literature to perform image combinations. For the purpose of this study, the Intensity, Hue and Saturation (IHS) cylindrical transformation seemed the more appropriated. The equations for the IHS colour transformation can be found in Harrison and Jupp (1990). Alternatively, the Brovey transformation was used as a second technique. The Brovey transformation equation is illustrated in Vrabel (1996).

Table 2: The fused images

Fused images	Imagery used	Transformation used
TMJC	Landsat TM 95 / JERS-1	IHS Cylindrical transformation
TMJB	Landsat TM 95 / JERS-1	Brovey transformation
TMEC	Landsat TM 95 / ERS-2	IHS Cylindrical transformation
TMEB	Landsat TM 95 / ERS-2	Brovey transformation

Classification of SAR and SAR-fused data is a research field that is being given increased attention (van der Sanden, 1997; Michelson *et al.*, 2000). Studies involving textural analysis-based classifications have obtained good results (van der Sanden, 1997) but operationally they are still time demanding and difficult to implement. Recently, new contextual classifiers based on Bayesian image segmentation algorithms have been created and are starting to be evaluated in practical applications. Michelson *et al.* (2000) compared an image segmetation algorithm (the SMAP), a neural network (based on the back propagation algorithm) and the maximum likelihood algorithm to perform land cover classification of Landsat TM, ERS-1 and fused ERS-1-Landsat TM imagery. The comparison of the overall classification accuracy indicated that the SMAP (57.1%) outperformed the maximum likelihood (52.4 %) which, in turn, outperformed the

neural network algorithm (51.2%). However, the maximum likelihood gave the highest accuracy for the forest classes using Landsat TM data. The Gaussian maximum likelihood is one of the most widely used algorithms for remote sensing data classification. It was the one used in this study because of its reliability and for being easier to operate if compared to the new classifiers described above. It assumes a normal distribution for the image values corresponding to the training data, allowing the description of the category response pattern by the mean vector and the covariance matrix (Lillesand and Kiefer, 1994).

The dendrometric (stand) parameters collected in the field, DBH and tree height, were used to stratify the forest training and the forest test set in two.

The cloud cover (and the correspondent shadow) gap areas on the Landsat TM 95 were masked manually, pixel by pixel. As a result, a bitmap layer delimiting the no-information areas was created (using PCI software) and added to each image to be classified.

The errors in a classified image can be assessed by using an error matrix (also called confusion matrix) (Congalton and Green, 1999). An error matrix compares the reference data (or ground truth), represented by the columns, with the classified data, represented by the rows. The accuracy for a given class is represented by the errors of inclusion ('commission' errors) and exclusion ('omission' error) of reference data units into the class (Congalton and Green, 1999). Similarly, the 'producer's' accuracy is the ratio between the number of correctly classified units of a given class and the total number of reference sampling units for this class, while the 'user's' accuracy is obtained by dividing the total number of correctly classified units by the total number of units (from all the classes) classified as this given class. The matrix's major diagonal indicates the agreement between the reference data and the classified data. Thus, the overall accuracy for a particular classified image is given by dividing the sum of the major diagonal's cells by the total number of reference sampling units (Congalton and Green, 1999).

Supervised classification was performed for the Landsat TM 95 alone, the two SAR data alone, and the four different fused Landsat TM 95 – SAR data using PCI ImageWorks. The maximum likelihood classifier was applied and the bitmap mask was used to avoid the TM 95 no-information areas.

The Landsat TM 96 (with no clouds), and the two fused images that had previously obtained the higher overall classification accuracy for one forest class, TMJC and TMEC, were classified in PCI ImageWorks, using the bitmap mask to classify only the area correspondent to the Landsat TM 95 no-information areas. The maximum likelihood classifier was employed together with the training sets for one forest class. The classified TM 96 image was then used as 'ground truth' information to generate tree test sets, using the stratified random sampling method.

Likewise the overall classification accuracy, the Kappa coefficient of agreement is a measure of accuracy. The Kappa value, or "KHAT" is defined by the subtraction of the chance of agreement from the observed accuracy divided by 1 minus the chance of agreement. The equation can be found in Congalton and Green (1999).

4 RESULTS AND DISCUSSION

Figures 1a and 1c show a subset of the speckle filtered and rectified JERS-1 and ERS-2 images. For both images the forest areas usually have a brighter tone than the non-forest. If the two images are compared to the Landsat TM 95 composite (Figure 1b), it can be noted that for the JERS-1 the contrast between forest and non-forest is higher than in the ERS-2. The net of gallery forests which are visible on the Landsat TM is clearly identified on the JERS-1 but not on the ERS-2 image.

The ERS-2 has short wavelength (C-band) and vertical (VV) polarisation results that the radar signal is dominantly scattered by the forest canopy. The JERS-1 has comparatively longer wavelength (L-band) and horizontal polarisation (HH). According to van der Sander (1997), the horizontally polarised radar waves penetrates deeper into a forest formation than the vertical polarisation. Similarly, the longer the wavelength, the deeper it penetrates into the forest. Therefore, it is expected that the JERS-1 signals can distinguish forest from non-forest (e.g. pasture) better than the ERS-2. Recent studies using SAR imagery for tropical forest mapping give support to this idea. Using SIR-C SAR imagery with different wavelengths to assess deforestation in the Brazilian amazon forest, Rignot *et al.* (1997) have found that the L-band has higher capability to separate forest from clearings if compared with the C-band. Similarly, Bijker and Hoekman (1996) observed that it's difficult to discriminate forest from non-forest when single date ERS-1 (with the same sensor characteristics as the ERS-2) images are used.

Both images were affected in more or less extends by the complex landforms of the area. The ERS-2, having a relatively low incidence angle (23 degrees), is very sensitive to terrain variations, which leads to shadowing (dark areas

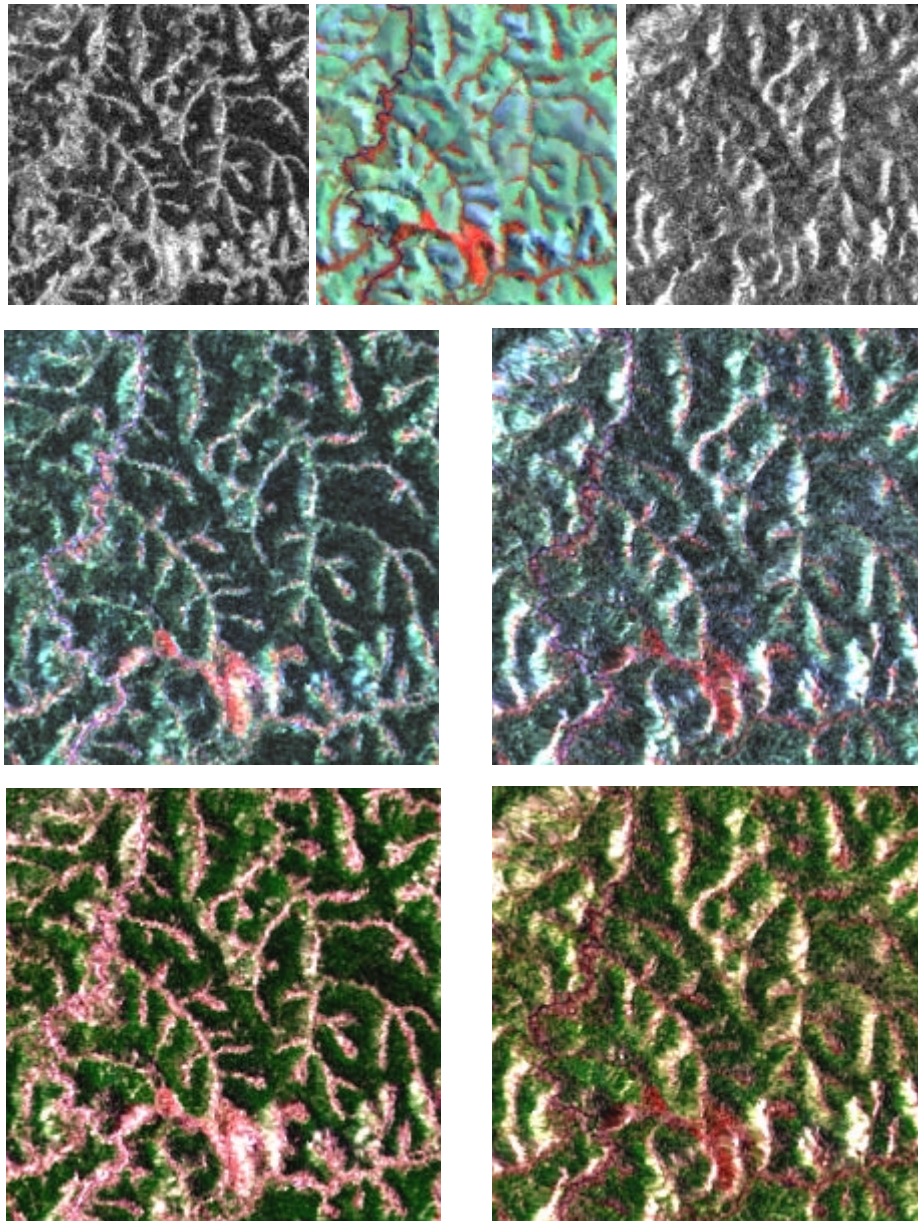


Figure 1: Single and fused image subsets comparison of an area with linear patches of gallery forest in the west of the study area. Starting from the upper left: JERS-1 (a), TM 95 453 (b), ERS-2 (c), fused Brovey TM 95/JERS-1 (d), fused Brovey TM95/ERS-2 (e), fused IHS cylindrical TM95/JERS-1 (f), fused IHS cylindrical TM95/ERS-2 (g).

on the image) for the hills that are facing away from the radar and layover (bright areas) for the hills facing towards the radar. This effect is less pronounced for the JERS-1 since it has a medium incidence angle (35 degrees).

Figures 1f and 1d show the subset of the fused Landsat TM 95 / JERS-1 images resulted from the IHS cylindrical transformation (TMJC) and from the Brovey transformation (TMJB) respectively. The distinction between forest and non-forest is clearer on the TMJC (IHS cylindrical transformation) than in the TMJB (Brovey transformation) image, giving to the first one an impression of greater sharpness. Figure 3-4 shows subsets of an area in the west of the study area where gallery forests and pasture predominates. For the TMJB (Figure 3-4d) the patches of gallery forest have a blurred appearance and their borderlines are difficult to identify. For the TMJC however, the bright reddish tone of the forest greatly contrasts with the pasture's dark green.

The image subsets obtained from the fusion of the Landsat TM with the ERS-2 image are displayed in figures 1-e and 1-g. TMEC is the image resulted from the IHS cylindrical transformation and TMEB, the one resulted from the Brovey transformation. The distinction made between the two fused TM / JERS-1 can also be applied to the fused Landsat TM /

ERS-2 images. TMEC is sharper than TMEB. However, the differences in contrast, saturation and sharpness between TMEC and TMEB are less pronounced than between TMJC and TMJB.

The previously described effects of topography on the SAR radiometry, layover and shadow are transmitted to the fused images since the Landsat TM intensity is substituted by the SAR intensity. For the layover effect, this is clear if Figures 1c (ERS-2), 1e (TMEB) and 1g (TMEC) are compared. The very bright areas (related to layover) on the ERS-2 image are also very bright on the fused images, independently on which type of transformation is used.

Visual comparison of the areas that corresponds to the Landsat TM cloud gaps on the fused images, indicated a clear superiority of the IHS cylindrical transformation over the Brovey transformation on the replacement of the information lost due to cloud cover. The cloud shadow areas (dark on the Landsat TM) appear with a dark purple tone on the Brovey transformed images. However, on the IHS cylindrical transformed images the same areas have a tonality that is similar to the areas where the cloud shadow is not present.

The classification using one forest class was performed to determine whether the data fusion can improve land cover classification accuracy for the study area if compared with the single Landsat TM. Table 3 summarizes the results of the Gaussian maximum-likelihood classification using one forest class. The user's, producer's and overall accuracies for each image (single and fused) were obtained from the error matrices. Moreover, the calculated Kappa coefficients and Kappa variances are indicated.

The classified Landsat TM 95 (TM951) presented an overall accuracy of 82.1%, with a Kappa coefficient of 0.618. The producer's accuracy achieved for the forest class is considerably higher (84.6% of the pixels were correctly classified) than the one achieved by the Eucalyptus plantation class (76.9%). The user's accuracy of the forest class is high, indicating that 91.7% of the area classified as forest is actually forest on the ground.

The two single SAR images achieved poor classification results. The JERS-1 achieved an overall accuracy of 50% a Kappa value of 0.087. In particular for the ERS-2, the classification resulted in an extremely low overall accuracy (5.7%) and a negative Kappa coefficient. The result reflects what was previously mentioned: the ERS-2 image not only had a lower contrast between forest and non-forest (due to its sensor characteristics) but also was more affected by the topographic variations (i.e. it has more layover and shadow areas than the JERS-1).

Table 3: Accuracy assessment summary for the classification with one forest class.

Cover Class	Classified Single Images			Classified fused images IHS cylindrical transf.		Classified fused images Brovey transf.	
	TM951 User Prod.	JERS1 User Prod.	ERS1 User Prod.	TMJC1 User Prod.	TMEC1 User Prod.	TMJB1 User Prod.	TMEB1 User Prod.
Forest	91.7 84.6	65.0 56.5	0 0	88.9 92.3	90.9 76.9	76.0 73.0	80.0 30.8
<i>Eucalyptus</i> Plantation	71.4 76.9	36.4 36.4	28.6 18.2	81.8 69.2	62.5 76.9	50.0 53.8	37.0 76.9
Overall Accuracy	82.1	50.0	5.7	84.6	76.9	66.7	46.2
Kappa Coefficient	0.61818	0.08723	-0.05	0.65385	0.52632	0.26415	0.1
Kappa Variance	0.01576	0.01292	0.05625	0.01533	0.01799	0.02575	0.04436

Despite the JERS-1 low classification accuracy, the TMJC1 (JERS-1 and IHS cylindrical transformation) fused image performed the highest overall classification accuracy (84.6%) and Kappa coefficient (0.654) among all the classified images. Moreover, its forest class producer's accuracy (92.3%) presented an increase of near 8% in relation to the same class accuracy for the TM951 (84.6%), for a similar value of forest user's accuracy in both images.

The second classification approach used two different sets of native forest subdivided from the original forest set to evaluate if the fused images could better differentiate forest classes structurally (the average stem volume was used as a parameter) different than the Landsat TM 95. Table 4 below summarizes the overall mapping accuracy and Kappa coefficients for each image classified using two forest classes. The user's, producer's and overall accuracies were obtained from error matrices.

The classification accuracies obtained are much lower if comparison is made with the classification carried out with one forest class. The best classification accuracy was achieved by the TMEC2 classified fused image. The result suggests that the distribution of the two forest strata might be related to the geomorphology of the area, given the ERS-2 greater sensitivity to terrain variations.

Table 4: Accuracy assessment summary for the classification using two forest classes.

Cover Class	Classified Single Images						Classified fused images IHS cylindrical transf.				Classified fused images Brovey transf.			
	TM952		JERS2		ERS2		TMJC2		TMEC2		TMJB2		TMEB2	
	User	Prod.	User	Prod.	User	Prod.	User	Prod.	User	Prod.	User	Prod.	User	Prod.
Forest A	46.1	46.1	33.3	8.3	0	0	33.3	23.1	53.8	53.8	42.9	46.2	30.0	23.1
Forest B	50.0	53.8	28.6	36.4	0	0	50.0	69.2	60.0	60.0	45.5	38.5	25.0	7.7
<i>Eucalyptus</i> Plantation	72.7	61.5	30.0	27.3	28.6	18.2	81.8	69.2	66.7	76.9	61.5	61.5	41.7	76.9
Overall Accuracy	53.9		23.6		5.7		53.8		59.0		48.7		35.9	
Kappa Coefficient	0.31646		-0.04938		-0.02758		0.31646		0.39241		0.30769		0.05063	
Kappa Variance	0.01394		0.01680		0.03273		0.01391		0.01318		0.01440		0.01819	

The classification accuracies for the areas that correspond to cloud cover were assessed throughout matrices. Table 5 summarises the results and adds the calculated Kappa coefficient and variance.

The results indicate similar classification accuracy for the two fused images. Although the test data sets used to assess the classification accuracy were based on the Landsat TM 96 classified image, an expressive classification accuracy was achieved for the forest class (around 60%). Attention is paid to the fact that the classification accuracy for the *Eucalyptus* class is null for both images. That is probably a result of extremely low signature separability between the forest class and the *Eucalyptus* class. As the number of sampling points used for the Forest training set was the half of the number for the training set, the Gaussian Maximum Likelihood classifier should had given ‘preference’ to the Forest signature instead of the *Eucalyptus* signature for classifying ‘doubt’ points.

Table 5: Summary of the accuracy assessment for the cloud gap areas classification.

Cover Class	Fused Images Classification for the Areas Correspondent to Cloud cover			
	TMJC1M		TMEC1M	
	User	Prod.	User	Prod.
Forest	55.4	65.7	90.9	67.1
<i>Eucalyptus</i> Plantation	0	0	0	0
Non-forest	56.7	54.3	54.8	48.6
Overall Accuracy	56.0		54.0	
Kappa Coefficient	0.175		0.13752	
Kappa Variance	0.00552		0.00582	

5 CONCLUSIONS AND RECOMMENDATIONS

The main problems encountered were related to the effects of topography on the SAR imagery (shadow and layover). These effects induced differences in the backscattered radar signals, which led to confusion of these differences with tonal differences from the different cover types. The consequence was the poor classification accuracy achieved by the SAR images.

Since the Landsat TM intensity is substituted by the SAR intensity during the data fusion process, the shadow and layover effects are transmitted to the fused images, generating the same confusion when the data is classified. However, even being affected by the shadow and layover, the TMJC image (fusion with JERS-1, using IHS cylindrical transformation) out-performed the Landsat TM classification accuracy. This is an indication that if some changes are made in the methodology, future research might lead to a significant improve in the classification results.

A visual comparison of the areas that corresponds to the Landsat TM cloud gaps on the fused images, indicated a clear superiority of the IHS cylindrical transformation over the Brovey transformation on the replacement of the information lost due to cloud cover. Although the test data sets used to assess the accuracy of the classification for the gap areas were based on the Landsat TM 96 classified image, a classification accuracy of about 60% was achieved for the forest class. However, the overall classification accuracy of zero percent for the *Eucalyptus* class indicates a low separability of this class from the forest class when the accuracy for the shadow areas is assessed.

All satellite (SAR and TM) imagery and ancillary data should be received with a considerable time before fieldwork so the SAR shadow and layover areas can be masked using the sensor parameters and a DEM for the area. The masking allows not only avoiding data collection in 'no-information areas' but it also can be used in image analysis techniques that compensate for the topographic effects. These techniques are still under development but had been already applied in some recent studies. Kellndorfer (1996) gives some directions on the methodology involved.

6 ACKNOWLEDGEMENTS

This paper is based on a MSc thesis carried out in the International Institute for Aerospace Survey and Earth Sciences (ITC). The Landscape Ecology Laboratory of the University of São Paulo (USP) supervised fieldwork activities. All the Landsat TM imagery used in this research was provided by the Brazilian National Institute for Space Research (INPE), with no cost. The PCI Corporation offered its EASI/PACE software package and direct support. The National Space Development Agency of Japan (NASDA) and the Dutch National Space Laboratory (NLR) provided the JERS-1 and the ERS-2 images at a research and demonstration pricing category. All digital maps were obtained from Telemar - Telecomunicações de Minas Gerais S.A. I would like to express my sincere gratitude to all the mentioned institutions.

7 REFERENCES

- Bijker, W. and Hoekman D. H. (1996).** "Monitoring of tropical rain forests and pastures with ERS-1. TREES ERS-1 94 study: LAM-8". In: van der Sander, J. J., Hoekman D. H., and Bijker, W., *Radar Remote Sensing of tropical rain forests: ERS-1 studies in Guyana and Colombia. Final report*. Delft (BCRS, Netherlands Remote Sensing Board) BCRS report no.96-09, pp. 29-23.
- Congalton, G.C. and Kass, G. (1999).** "Assessing the accuracy of remotely sensed data: principles and practices". Lewis Publishers, New York, 137 pages..
- Hudson, W. D. and Ramm, C. W. (1987).** "Correct formulation of the Kappa coefficient of agreement". *Photogrammetric Engineering & Remote Sensing*, Vol.53, No.4, pp. 421-422.
- Harrison, B. A. and Jupp, D. L. B. (1990).**"Introduction to image processing",pp.256. In "microBRIAN Resource Manual", (eds). CSIRO Publications, Melbourne, Australia
- IUCN (1996).**"The conservation atlas of tropical forests - the Americas". Simon and Schuster, New York, 335 pages.
- Kellndorfer, J., Dobson, M.C., Ulaby F.T. (1996).** "Geocoding for Classification of ERS/JERS-1 SAR Composites". In: *Proc. IGARSS 96*, Lincoln, Nebraska, USA, pp. 2335-2337.
- Lee, J. S. (1980).** "Digital image enhancement and noise filtering by use of local statistics". *IEEE Transactions on Pattern Analysis and Machine Intelligence*, Vol.2, No.2, pp. 165-168.
- Lillesand, T. M. and Kiefer, R. W. (1994).**"Remote sensing and image interpretation". 3rd. Wiley & Sons, New York, 750 pages.
- Lopes, A., Nezry, E., Touzi, R. and Laur, H. (1993).** "Structure detection and statistical adaptive filtering in SAR images". *International Journal of Remote Sensing*, Vol.14, pp. 1735-1758.
- Michelson, D. B., Liljeberg, B.M. and Pilesjö, P. (2000).** "Comparison of algorithms classifying Swedish landcover using Landsat TM and ERS-1 SAR data". *Remote sensing of environment*, Vol.71, No.1, pp. 1-15.
- Oliveira-Filho, A. T. and Ratter, J. A. (1995).** "A study of the origin of central Brazilian forests by the analysis of plant species distribution patterns". *Edinburgh Journal of Botany*, Vol.52, No.2, pp. 141-194.
- Pohl, C. (1996).**"Geometric aspects of multisensor image fusion for topographic map updating in the humid tropics.". ITC publication No. 39, Enschede, The Netherlands, 160 pages.
- Rignot, E., Salas, W. D. and Skole, D. L. (1997).** " Mapping deforestation and secondary growth in Rondonia, Brazil, using imaging radar and Thematic Mapper data". *Remote Sensing of Environmen*, Vol.59, pp. 167-179.
- SOS, Mata Atlântica and INPE (1993).**"Atlas da evolução dos remanescentes florestais e ecossistemas associados do domínio da Mata Atlântica no período 1985-1990". SOS Mata Atlântica and Instituto de Pesquisas Espaciais, São Paulo, Brazil.
- SOS, Mata Atlântica, INPE and ISA (1998).**"Atlas da evolução dos remanescentes florestais e ecossistemas associados do domínio da Mata Atlântica no período 1990-1995". SOS Mata Atlântica, Instituto de Pesquisas Espaciais and Instituto Socioambiental, São Paulo, Brazil.
- van der Sanden, J. J. (1997).**"Radar remote sensing to support tropical forest management". Wageningen Agricultural University, Tropembos-Guyana Series 5, Wageningen, The Netherlands, 330 pages.
- Veloso, H. V., Filho, A. L. R. R. and Lima, J. C. A. (1991).**"Classificação da vegetação brasileira, adaptada a um sistema universal". IBGE, Departamento de Recursos Naturais e Estudos Ambientais, Rio de Janeiro, 124 pages.
- Vrabel, J. (1996)** "Multispectral Imagery Band Sharpening Study". *Photogrammetric engineering and remote sensing*, Vol.62, pp. 1075-1084.